

## Experimental Study of Molten Metal Penetration and Freezing Behavior in Pin-Bundle Geometry

by

M. Kabir HOSSAIN\*, Yusuke HIMURO\*, Koji MORITA\*\*,  
Kiyoshi NAKAGAWA\*\*\*, Tatsuya MATSUMOTO†, Kenji FUKUDA†† and  
Werner MASCHKE†††

(Received November 4, 2008)

### Abstract

Molten metal penetration and freezing phenomena were studied during the interaction with reactor core structures from the view point of the safety analysis of heavy liquid metal cooled reactor. For the determination of the fundamental mechanisms underlying the penetration and freezing behavior of molten metal flowing through a seven-pin channel was the main objectives of this study. The present series of simulant experiments, therefore, has been performed to study the freezing phenomena of molten metal (wood's metal) which focus on fuel pin-bundle geometry under the various thermal conditions of molten metal and pins. The liquid penetration length into the flow channel and the proportion of adhered frozen metal onto the pin surfaces were measured in the present series of experiments. Visual information was also obtained by using a digital video camera. The comparison between the atmosphere and the water-coolant experiments shows that characteristics of penetration and freezing behavior will significantly change due to heat transfer from melt to coolant. The present results will be utilized to create a relevant database for the verification of reactor safety analysis codes.

**Keywords:** Liquid metal cooled reactor, Penetration length, Reactor safety, Freezing behavior

### 1. Introduction

Analysis of a hypothetical core disruptive accident (CDA) is of great concern for the safe design of future generation reactors like liquid metal cooled reactor (LMR). The streaming, freezing and blockage phenomena of molten fuel in the core structures during the transition phase of a CDA have been important areas of LMR safety research. In a transition phase, the subassemblies are overheated and a gradual core melt-down occurs with fuel and steel melting-in to form a molten pool. A multi-component, multi-phase flow arises in the core consisting of fuel fragments, molten fuel and steel, fission gas and liquid and vaporized coolant. Should an early discharge from the core region occur, the possibility of neutronic ceasing increases to eliminate a recriticality. Otherwise, a formation of flow blockage in blanket regions can bottle up the core and the molten pool propagates in whole-core scale arising the tremendous feedback on the further course of accidents<sup>1)</sup>. It was assessed in the analysis that in order to assure permanently subcritical condition (i.e., no power burst could be expected any more) in a CDA sequence, more than 30% of the fuel inventory had to be discharged from the core region and subsequent migration inside the reactor vessel<sup>2-5)</sup>. Thus the discharge/penetration and freezing of molten core materials into colder structures are the key phenomena for the analysis of transition phase.

**Figure 1** shows the postulated CDA sequences of heavy LMR whereas **Fig. 2** reveals the

---

\* Graduate Student, Department of Applied Quantum Physics & Nuclear Engineering

\*\* Associate Professor, Department of Applied Quantum Physics & Nuclear Engineering

\*\*\* Technical Assistant, Department of Applied Quantum Physics & Nuclear Engineering

† Assistant Professor, Department of Applied Quantum Physics & Nuclear Engineering

†† Professor, Department of Applied Quantum Physics & Nuclear Engineering

††† Institute for Nuclear and Energy Technologies, Forschungszentrum Karlsruhe, Germany

predicted schematic view of CDA phenomenology of heavy LMR. It is anticipated that the penetration of molten fuel into the open flow channels is limited due to the freezing and crust deposition, creating plugs that eventually will occlude the flow paths. The freezing process depends on a variety of factors, like the melt's flow regime, the crust's stability against thermal and hoop stress, crust entrainment into the main flow and wall structure integrity or melting and injection into the main flow<sup>6)</sup>. However, the extensive design effort for accident prevention, including advanced passive safety features, will make the occurrence of such an event extremely unlikely in future LMR commercialization. The importance of severe accidents is still emphasized from the viewpoint of safety design and evaluation to appropriately mitigate and accommodate the consequences and thereby to minimize the risk to the public<sup>7)</sup>.

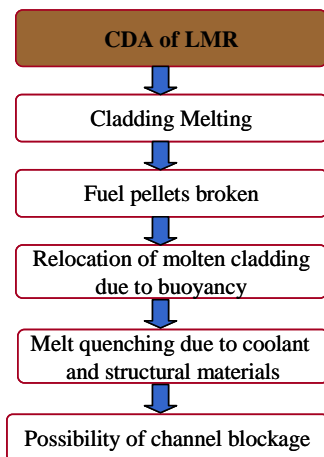


Fig.1 CDA sequences of heavy liquid metal cooled reactor.

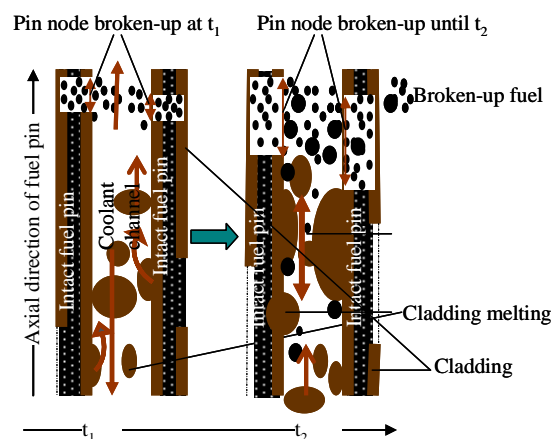


Fig. 2 Schematic view of the sequences of material relocation during CDA in a heavy LMR.

Several series of experiments (in-and out-of-pile) on hydrodynamic aspects of molten fuel penetration into the reactor core structures have been studied extensively in the past<sup>1-3, 6, 8-11)</sup>. Their studies presented basic experimental data for materials flowing and freezing where defined quantities of melt were injected into flow structures. Spencer *et al.*<sup>10)</sup> have done a series of pin bundle (7 and 37-pins) experiments, and they found molten fuel (mixture of molten UO<sub>2</sub> and molybdenum metal) to freeze with blockage formation within the pin bundles. Menzenhauer *et al.*<sup>1)</sup> have done out-of-pile experiments with thermite in pin bundle geometry (7 and 19-pins) and observed tight blockages in the upper and lower breeder zones. However, understanding of the phenomenology of the transition phase is still limited partly due to difficulties in conducting related experiments to delineate the accidents. Most of the research has been concerned with the freezing of molten fuel in the frozen channel without liquid coolant condition. This is because during CDA of sodium cooled reactor, coolant will vaporize and disappear due to good heat transfer from stainless steel and fuel in solid and liquid phases, of which temperature can be higher than boiling point of liquid sodium (880 °C). But in a heavy liquid metal cooled reactor, coolant (Pb or Pb/Bi eutectic) with high boiling point (1750 °C or 1670 °C)<sup>12)</sup> may exist even though the stainless steel melts at 1430 °C.

Recently, a substantial attention has been drawn on melting freezing experiment in presence of liquid coolant in the flow channel from the view point of LMR safety. Rahman *et al.*<sup>13)</sup> studied the molten metal freezing phenomena and observed distinct freezing modes of molten metal in water coolant condition. Their studies were to investigate the fundamental freezing behavior of molten metal during penetrating onto a metal structure, but were not performed for pin-bundle geometry, which is one of the main discharge paths of the molten materials during CDAs. The present work is an extension of their study to identify the molten metal penetration and freezing in pin bundle geometry with the verification of the models and methods for the numerical simulation.

The purpose of the present study is to determine the fundamental mechanisms underlying the penetration and freezing behavior of molten metal flowing through a seven-pin channel. In particular, the present study was conducted to observe the behavior of melt freezing and penetration in seven-pin channel under the water coolant conditions. To achieve the aim of this study, a series of simulant experiments has been performed to investigate and characterize the interactions among flowing molten metal (wood's metal), stainless steel pins and coolant (water). The experiments focus on pin-bundle geometry under the various thermal conditions of molten metal, coolant and pins. The data obtained from the experiments will be utilized to establish a reference database for the verification of reactor safety analysis codes.

## 2. Seven-pin Experiment

### 2.1 Experimental set-up

A schematic diagram of the experimental apparatus is shown in **Fig. 3**. This equipment consists of a melt tank section and a flow channel section. The former is used to melt and inject the simulant material and the latter is used to observe the penetration and freezing behavior of the molten metal. The melt tank is made by Pyrex glass into which melt is poured. The lengths of the melt tank's neck and the channel sections are 8 and 50 cm, respectively. A plug, made by Teflon, is connected to the top of the melt tank's neck to make a transient melt pool by pulling-up the plug. Thus the transient melt pool is set at the top of the channel part separated by a thin layer ( $\sim 1.5$  mm) of wood's metal. This layer is for the smooth injection of melt into the channel. Twenty one k-type (chromel-alumel) thermocouples are connected to the pins and melt tank to measure the temperature of the flowing melt and pins. The pins are made of stainless steel and outer tubes are made of Pyrex glass for visual observation. The set-up is positioned on a basement made of stainless steel and supported by a fixed stand. Hydraulic parameters to execute this series of experiments are summarized in **Table 1**.

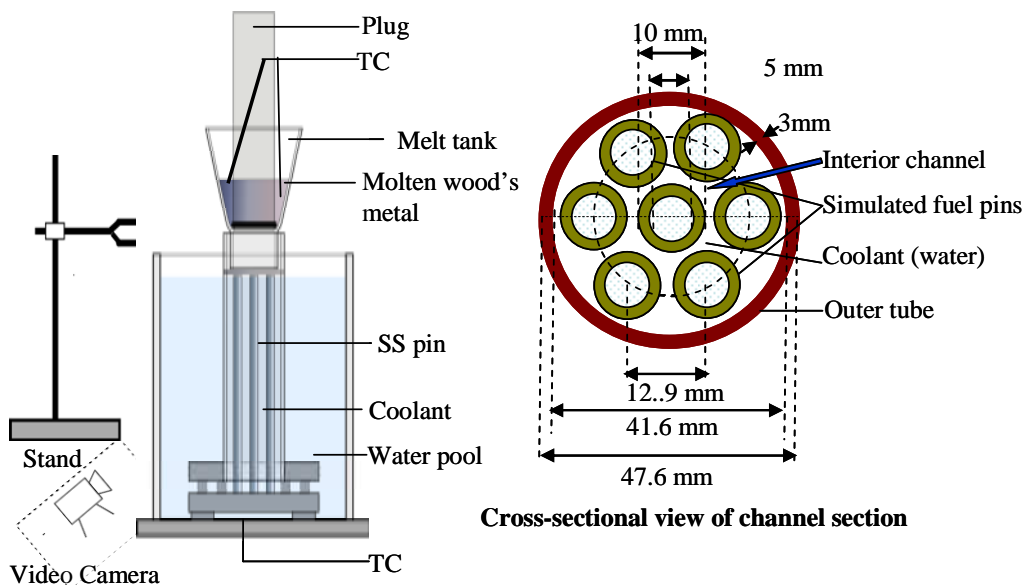


**Fig. 3** Schematic diagram of experimental apparatus.

The water pool, which is a cylindrical open-topped box measuring 570 mm in height  $\times$  300 mm in dia., is made of Pyrex glass for the purpose of visual observation. A thermocouple sensor is used to control the water temperature at a desired level. During experiments in the atmosphere, the water pool was absent. A digital video camera was used to record the video images of the melt as it falls onto the pins.

Using this apparatus, a series of melting-freezing experiments is conducted involving the interaction of molten metal with pins using air and water as coolant so as to simulate the fundamental freezing behavior of molten metal during core meltdown of LMRs under CDA. Out of

a series of experiments, some good results have been selected based on uniform melt injection and length of penetration are presented in this paper. The purpose of this experimental series is to study the penetration and freezing behavior of molten metal as it freezes into/on the core structure and to determine some physical parameters such as a penetration length and an amount of frozen metal adhering to the core structure.

**Table 1** Hydraulic parameters of a seven-pin channel experiment.

Parameter	Value
Number of fuel-pin	7
Outer pin diameter (mm)	10
Inner pin diameter (mm)	5
Pin pitch (mm)	12.9
Hydraulic diameter (mm)	8.34
Inner diameter of the outer tube (mm)	41.6
Outer diameter of the outer tube (mm)	47.6
Thickness of the outer tube (mm)	3

In the present study, wood's metal with weight composition of Bi 60 %, Sn 20 % and In 20 % is used as a simulant molten metal. Its melting point is low (78.8 °C) and boiling point is high (1760 °C). Considering the application of the experimental results to the nuclear reactor situation, low melting wood's metal is chosen since its density and thermal conductivity are similar to those of molten stainless steel which would be one of the disrupted core materials. The melting point is lower than the boiling point of water at the atmospheric pressure. Some of the physical properties of wood's metal and stainless steel are given in **Table 2**.

**Table 2** Physical properties of wood's metal<sup>13, 14)</sup> and stainless steel<sup>15, 16)</sup>.

Parameter	Wood's metal	Stainless steel (Grade 316L)
Melting point (°C)	78.8	1430
Density (kg/m <sup>3</sup> )	8100	8000
Thermal conductivity (W/mK)	11.1	16.2
Specific heat (J/kgK)	150	530
Kinematic viscosity (m <sup>2</sup> /s)	$2 \times 10^{-7}$	$1.97 \times 10^{-7}$
Latent heat of fusion (J/kg)	$2.53 \times 10^4$	$3.39 \times 10^5$
Surface tension (N/m)	1.0	1.131
Weight composition	Bi (60 %), Sn (20 %) and In (20 %)	Fe (69 %), Cr (17 %), Ni (12 %) and Mo (2 %)

## 2.2 Experimental procedure

Using two types of surrounding fluid (air and water), the present series of experiments are conducted in two steps. In the atmosphere experiments, the thin layer of solid wood's metal is made at first on the bottom of the melt tank's neck by liquid wood's metal. Then the flow channel structure (pins) is heated by blowing hot air from the top and bottom of the channel. The temperature of the pins is monitored using a computerized thermocouple device to get the specified pin temperature. At the same time, a specified amount of wood's metal is heated by an electric heater; the temperature of the melt is monitored by a digital thermometer. The temperature of the melt, transferred to the melt tank, is also measured to achieve a desired temperature. After reaching the desired melt and pin temperature, the plug is pulled-up and melt starts to flow. The melt makes a transient melt pool on the top of the flow channel since a thin solid wood's metal layer is there, and by melting this layer, melt is injected into the flow channel. The molten metal flows down from the top of the flow channel due to gravitational acceleration.

**Table 3** Experimental conditions.

Melt mass (g)	Pin/water temperature (°C)	Melt temperature (°C)
215/325	25-55	100
215	25	90-132

In water coolant experiments, the set-ups mentioned above are installed in the water pool. An amount of hot water at a desired temperature was poured in the water pool and is monitored by a digital thermometer. A stirrer is employed to create the uniform water temperature throughout the pool. After getting the specified water temperature, the molten metal is prepared as mentioned above and is investigated the freezing and penetration behavior of the molten metal into the channel. Experiments (in air and water) are performed by changing the temperature and mass of the molten metal and the temperature of pins as well as water. The experimental conditions are summarized in **Table 3**.

The penetration of molten metal during the interaction with the structures and the coolant, flowing behavior are observed by using a digital video camera. The adhered frozen layer and the other fragments like debris are collected after each experiment. The penetration length, which is the average length of the molten metal that penetrates into the channel and finally adheres to the pin surfaces, is measured. In both the air and water cooled conditions, experiments are carried out at the atmospheric pressure.

### 3. Results and Discussion

#### 3.1 Experimental observation

Effects of the melt penetration and the freezing behavior are observed by varying the melt mass and temperature of molten metal and pins. A most interesting and significant result is typified in **Fig. 4** that the molten metal does not wet the solid stainless steel pins surfaces. The no wetting is evidenced by observing the convex shapes of the slugs of frozen metal, which were easily removed from the pins in posttest examination; the solidified metal was not “welded” to the pin surface. The surface of the solidified metal was rough in texture containing numerous cavities and dents were there as shown in **Fig 4**. The occurrence of such surface cavities has been noted by previous researchers including Kölling and Grigull <sup>17)</sup> for the freezing of flowing molten lead and has been drawn from results of Kuhn, Möschke, and Werle <sup>18)</sup> for molten iron injected into quartz glass tubes. That has been also implied by the results of Sienicki et. al <sup>3)</sup>, Spencer et. al. <sup>2)</sup> for molten stainless steel and nickel injected into stainless steel tube filled with argon gas.

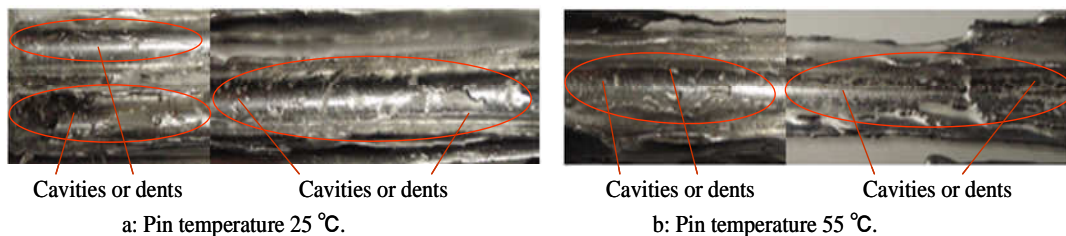


**Fig. 4** Photographs of adhered frozen metal in the flow channel addressing cavities and dents.

The typical freezing behaviors of molten metal in the channel in the atmosphere are depicted in **Fig. 5**. In this figure, photographs of frozen metal of six experimental observations are presented in three cases. For each case, the photographs ‘a’ and ‘b’ show the results of lower and higher pin/melt temperature conditions, respectively. It should be noted that the photographs of ‘b’ are enlarged in comparison with those of ‘a’. In Case-1, -2 and -3, the upstream part of the frozen metal in the lower temperature cases (photographs ‘a’) is thicker and wider than that in the higher temperature cases. This result can be explained that during hot melt flowing into the channels, the most of the melt froze at the upper part of the pins due to rapid loss of its significant amount of latent heat. The frozen metal became thicker and wider. However, for the case of higher temperatures of pins and melt, the time getting freezing point of melt was bit late, hence, the molten metal penetrated longer distance, and became thinner since the same amounts of melt were ejected in the both lower and higher temperature cases.

**Figure 6** typifies the experimental results under the water coolant conditions at different temperatures of water and melt. In this figure, photographs of frozen metal of nine experimental observations are presented in three cases. In Case-1, -2 and -3, each photograph shows the results

from the case of different temperature between water and melt, respectively. It is observed from these photographs that when hot melt passed through channels in presence of water, a part of molten metal was frozen and quenched immediately in the upper part of the channel, where a significant amount of molten metal broke up and fell down in different fragments as debris of various sizes. This is because of a drastic increase in effective viscosity of melt flowing due to rapid decrease in melt temperature where smooth heat transfer occurred from hot molten metal to cold water and pins. Although the shape and size of the debris are varies from test to test, small debris looks close to spherical shape. The edges of large fragments are keen and their surfaces are rough but those of small debris are smooth.

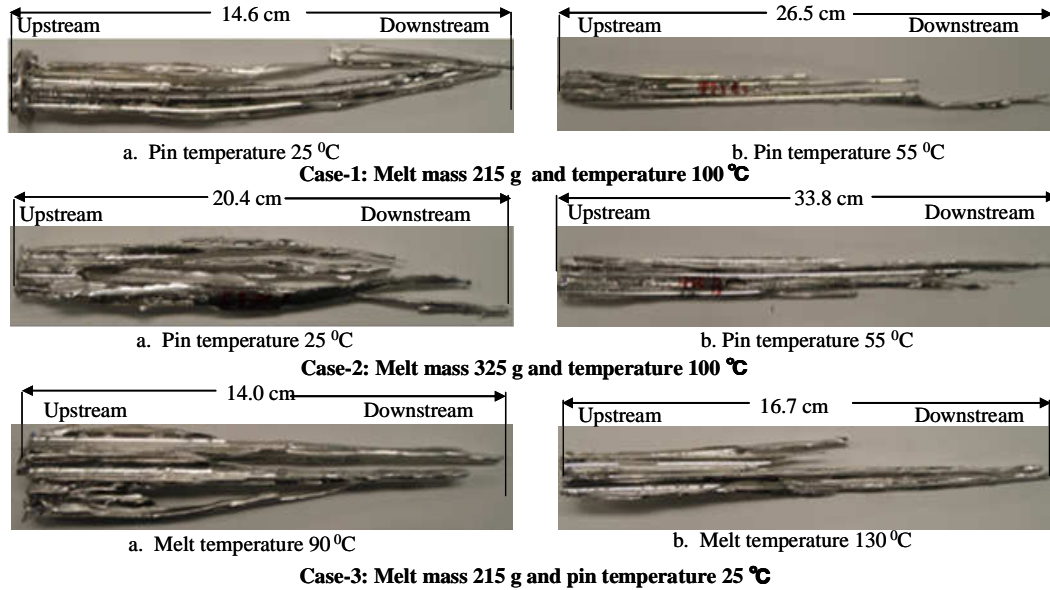


**Fig. 5** Photographs of frozen metal observed in the flow channels in the atmosphere by changing the melt mass and the temperature of molten metal and pins.

The debris observed in the water coolant experiments is comparable well with those found by Rahman et al.<sup>13)</sup>, Abe et al.<sup>19)</sup> and Bang et al.<sup>14)</sup>. They also used Wood's metal as the molten metal at a temperature of around 90-100 °C and the temperature of their water pool was 50 °C.

It is also seen from the photographs in **Fig. 6** that the adhered frozen metal on the pin surfaces became thinner and the length of frozen metal decreased gradually with increasing the temperature of water and molten metal. This was because the effective viscosity decreased gradually as the water/melt temperature increased, and the frozen metal adhered on the pin surfaces became unstable and broken up, and then fell down as debris. Some instability was observed around water temperatures 32 and 40 °C in Case-2, where the frozen metal and debris making tight blockage in the channel jumbled and the penetration length elongated. This behavior will be explained in Subsection 3.2.1. At low water temperatures, some debris became long and thin like a pencil, whereas at high temperatures such debris disappeared and the most of debris became smaller. The velocity and temperature of the surrounding fluid at the time of solidification may affect the shape. Beside these, some instability was also found which might be due to initial inertia of the melt and another hydrodynamic interaction mechanism.

### 3.2 Quantitative measurements

#### 3.2.1 Penetration length

Penetration length is the average length of molten metal into the channels and adhered finally onto the pin surfaces. The maximum length was measured at all six sub-channels and then the average length was taken as the penetration length. The average penetration length of molten metal in the channels is plotted as a function of pin, and the melt temperature in air atmosphere is shown in **Figs. 7** and **8**, respectively.

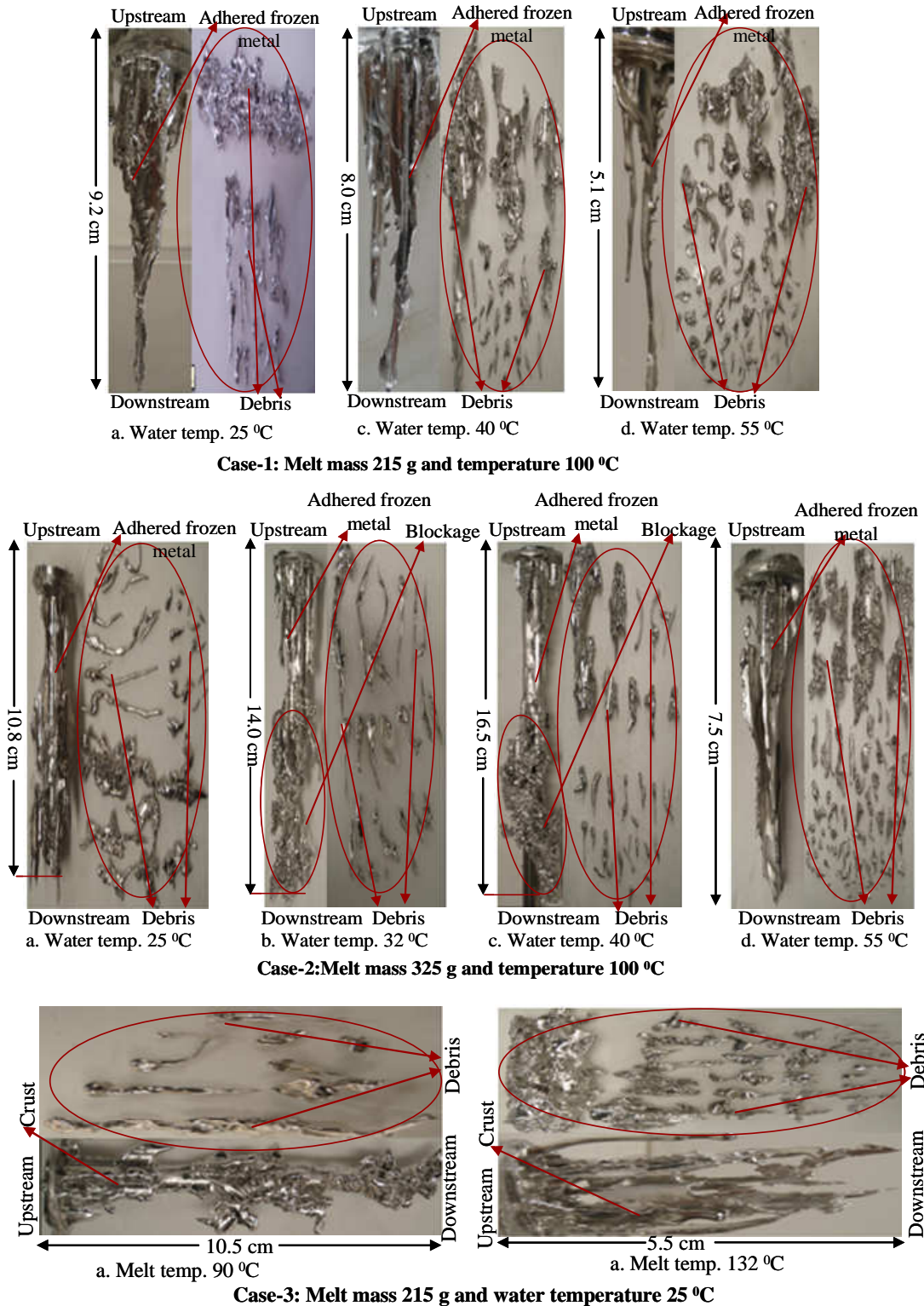


**Fig. 6** Photographs of frozen metal observed in the flow channels in water coolant condition by changing the melt mass and the temperature of water and molten metal.

It is clearly seen from **Fig. 7** that penetration length increases with increasing the pin temperature. This was because heat transfer from molten metal to pin structures, at high pin temperatures

became slow and the molten metal reached its freezing point bit late that resulted in melt long penetration. Comparing the penetration lengths between low mass (215 g) and high mass (325 g) cases we predicted that the penetration length for the high mass case would become longer than for the other case. It can be seen from **Fig. 8** that the penetration length varied slightly with melt temperature. **Figures 7 and 8** reveal that the variation of penetration lengths is marginal for melt temperature but the penetration length (in **Fig 7**) varies significantly with pin temperature.

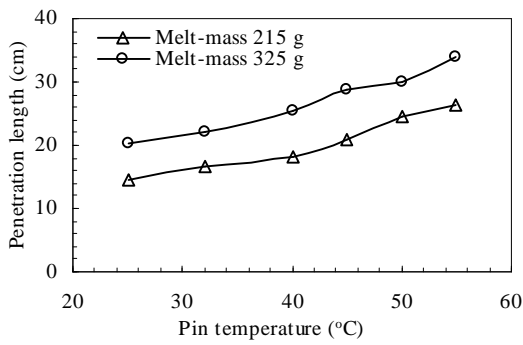


**Fig. 7** Average penetration length of molten metal in the atmosphere at different pin temperature (melt temp.: 100 °C).

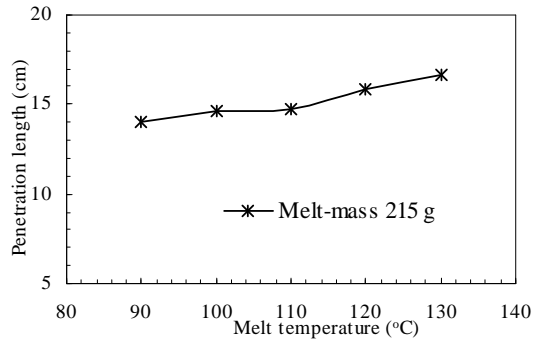


**Fig. 8** Average penetration length of molten metal in the atmosphere at different melt temperature (pin temp.: 25 °C).

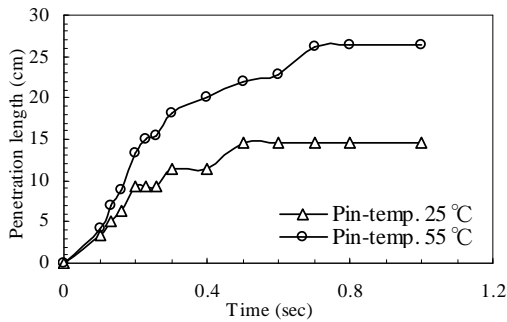


**Fig. 9** Transient penetration length of molten metal in the atmosphere at different pin temperature (melt mass: 215 g).

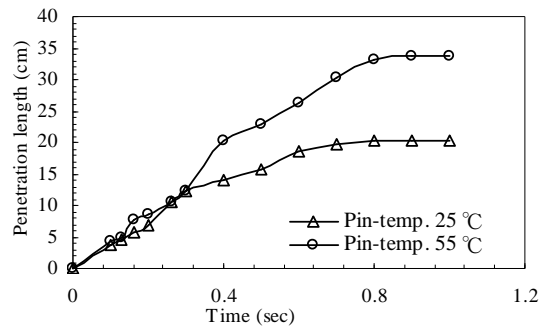


**Fig. 10** Transient penetration length of molten metal in the atmosphere at different pin temperature (melt mass: 325 g).

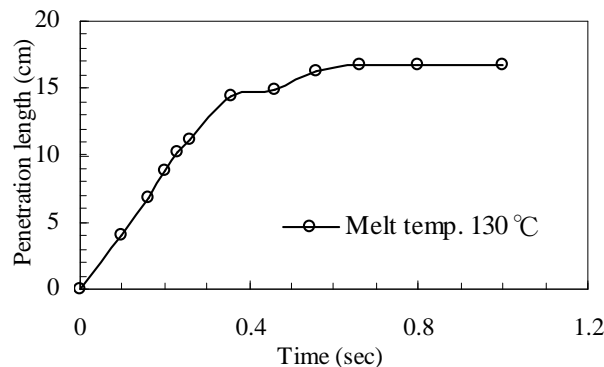


**Fig. 11** Transient penetration length of molten metal in the atmosphere (pin temp.: 25 °C, melt temp.: 130 °C, melt mass: 215 g).

**Figures 9 and 10** show the transient penetration length of molten metal into the channels in the atmosphere for different conditions of simulant melt mass. The result in the high melt temperature case is plotted in **Fig. 11**. In the experiments, the transient positions of melt penetration were determined from thermocouple signals as well as the recording images taken by the digital video camera. It can be seen from **Figs. 9 and 10** that transient penetration length increases with increasing the pin temperature. It is also illustrated in these figures that the total time of freezing of molten metal is earlier at the low pin temperature (25 °C) and the small amount of molten metal (215 g) than at the high pin temperature (55 °C) and the large amount of molten metal (325 g).

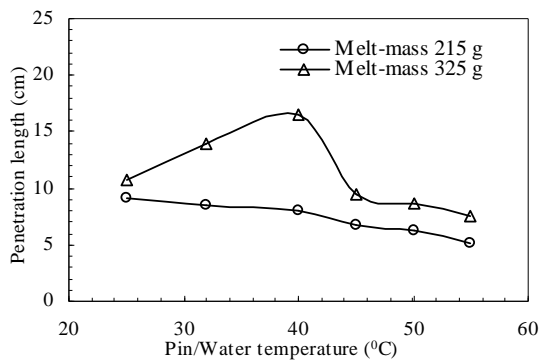


**Fig. 12** Average penetration length of molten metal in presence of water coolant at different water temperatures (melt temp.: 100 °C).

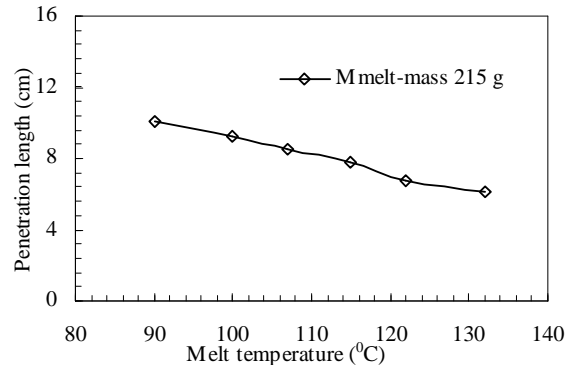


**Fig. 13** Average penetration length of molten metal in presence of water coolant at different melt temperatures (pin temp.: 25 °C).

The penetration lengths of molten metal in the water coolant experiments are plotted against water and melt temperatures as shown in **Figs. 12 and 13**, respectively. It is worth mentioning that compared with the atmosphere experiments, rather short penetration length is found in these results. This was because rapid cooling occurred due to smooth heat transfer to water and pins and thus the molten metal froze into debris. As a result, the short penetration length was achieved. It is observed in these figures that in the case of molten metal with 215 g the penetration length slightly decreased with increasing the water and melt temperature. At a low water temperature, the pin temperature was also low and the heat transfer from the molten metal to the pin structures was dominant which results in more thick and tight adhered frozen layer formation on the pin surfaces and thus longer penetration. With increasing the water/melt temperatures, the adhered frozen metal became unstable (due to gradual decrease in effective viscosity) and broke out and fell down as debris. As a result, the rate of debris formation increased and the penetration length became slightly short.

As can be seen also from **Fig. 12**, in the case of molten metal with 325 g, the melt penetration length significantly increases initially with increasing the water temperature and then decreases with further increasing the water temperature. It finally shows the similar trend in the case of the molten metal with 215 g. This was because with increasing the water temperature the broken adhered frozen metal or debris was entrapped into the channels at a few centimeters below the main adhered frozen metal, and it made blockage with debris. While the molten metal from melt pool was further flowed into the channel, the melt and the debris could not flow down more due to the blockage. As a result, the broken entrapped frozen metal and the main frozen metal made connection and appears elongated frozen metal length. If we further increased the water temperature, broken frozen metal and debris became small and slide down more than before or accumulated at the basement of the channel without making blockage. Therefore, the resultant trend of melt penetration length became similar to that of the low mass case. However, in the case of the molten metal with 215 g, the broken adhered metal was also entrapped into the channel at low water temperature but the liquid metal in the reservoir was not sufficient to make connection with the original frozen metal and the broken entrapped frozen metal. As a result, no increasing penetration phenomena were observed in the low mass case.

### 3.2.2. Mass distribution

The total mass (215 g, injected 80%) distributions of molten metal in the frozen channel in presence of water coolant are depicted in **Figs. 14** and **15**, with respect to the water temperature and the melt temperature, respectively. It is observed in the figures that the amount of adhered frozen metal decreases with increasing water or melt temperature while the amount of particle formation increases with increasing the temperatures of water and molten metal. This was because with increasing the water or melt temperature, the adhered frozen metal became unstable (due to gradual decrease in effective viscosity) and then broke out and fell down as debris. As a result, the amount of debris formation increased. The maximum amount of particle formation as debris was found 94 % and 81 % for the combination of water and melt temperatures of 55 and 100 °C and 25 and 132 °C, respectively. The enhancement of particle formation in presence of water coolant was due to a drastic increase in effective viscosity of melt due to rapid decrease in melt temperature because of smooth heat transfer. Some inconsistencies are also observed there, however. These might be due to improper operation of melt injection or some other interaction mechanisms such as buoyancy or increasing viscosity.

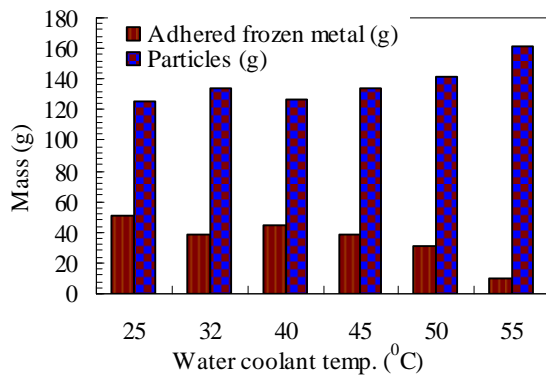


**Fig. 14** Total mass distribution in the frozen channel in presence of water coolant at different water temperatures (melt temp.: 100 °C).

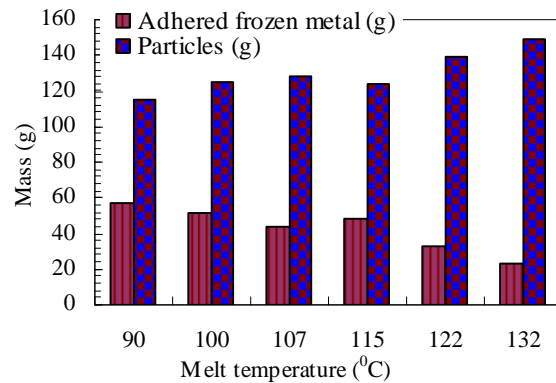


**Fig. 15** Total mass distribution in the frozen channel in presence of water coolant at different melt temperatures (water temp.: 25 °C).

### 3.3 Comparison between air atmosphere and water coolant experiments

In comparison of the freezing behavior of molten metal in the atmosphere and the water coolant experiments, it is obvious that the most of the frozen metal adhered to the pin surfaces was thick and wide at the upstream while thin at the downstream in the atmosphere experiments. On the other hand, in water coolant experiments, the most of the molten metal froze into particles as debris, and the adhered frozen metal became thin and short. The uniform shape with good adherence of frozen metal was also found in the atmosphere experiments, whereas in the water coolant experiments, only a small fraction of the molten metal froze onto the pin surfaces and a significant amount of molten metal broke and fell down as debris where debris was of various sizes and fragments were of broken adhered frozen metal. So in the atmosphere cases we found only one freezing mode as frozen on the pin surfaces, whereas in the water coolant cases two modes like adhered frozen metal on the pin surfaces and dominant particle formation were observed.

In the atmosphere experiments, the penetration length tends to increase gradually with increasing the pin and melt temperatures and the adhered frozen metal become thinner due to long penetration. In the water coolant experiments using small amount of melt, the penetration length decreased slightly with increasing the temperatures of the melt and pin as well as the coolant, and the adhered frozen metal became thinner due to particle formation and the adhered metal broken. The maximum penetration length of the molten metal was found to be 11 cm in the water coolant experiments, whereas in the atmosphere experiments it was found to be 34 cm, about 3 times greater than in the water coolant experiment. In the atmosphere experiments, the most of the frozen metal adhered to the structure, while in the water coolant experiments 73 – 94 % of the molten

metal froze into the structure as debris depending on the test conditions.

#### 4. Conclusions

A series of melt penetration and freezing experiments in a seven-pin channel under the atmosphere and the water coolant conditions was performed in order to investigate the freezing phenomena. There was no evidence that the molten wood's metal wet the pin surfaces as revealed by the convex shapes observed on solidified metal slugs which were easily removed from the pins as well as the appearance of cavities or dents on the frozen metal inner surfaces.

In the atmosphere experiments, the penetration length was found to be increased significantly with increasing the pin temperature. On the other hand, it decreased slightly with increasing the water temperature as well as the pin temperature in the water coolant experiments using the small amount of melt, where the short penetration length was found. The penetration length changed (increases in the air and decreases in the water) slightly with the melt temperature. This indicates that the effect of melt temperature on penetration length is not significant under the present experimental conditions. In the atmosphere experiments, the upstream of the frozen layer on the pin surfaces became thicker and wider than the downstream.

From the visual information of frozen metal in the water coolant experiments, it was found that only a small fraction of the molten metal froze onto the pin surfaces and a significant proportion of frozen metal broke up and fell down in different fragments including debris of various sizes. In addition, high instability was found in the case of water coolant experiments, which might owe to buoyancy, increasing viscosity and some other interaction mechanisms.

In comparison of the atmosphere experiments the most of the frozen metal adhered onto the pin surfaces and the shape of the frozen metal was thicker and wider with good adherence than in the water coolant experiments. In the water coolant experiments, it was found that the most of the frozen metal broke up and fell down as debris and only a small fraction was adhered on the pin surface and the shape of the frozen metal became thin and non-uniform.

The data obtained in the present series of experiments can be expected to be applied to utilize a reference database for the verification of reactor safety analysis codes.

#### References

- 1) P. Menzenhauer, W. Peppeler, et al.; Material movement, relocation and inter-subassembly propagation in bundles under simulated accident conditions (out-of-pile experiments with thermite), Science and technology of fast reactor safety, BNES, London, pp. 373-379, (1986).
- 2) B. W. Spencer, R. J. Wilson, et al.; Results of recent reactor-material tests on dispersal of oxide fuel from a disrupted core, Proceedings of the International Topical Meeting on Fast Reactor Safety, Knoxville, Tennessee, pp.877-882, (1985).
- 3) J. J. Sienicki, B. W. Spencer, et al.; Freezing controlled penetration of molten metals flowing through stainless steel tubes," ANS Proc. of 1985 National Heat Transfer Conference, Denver, pp. 245-254, (1985).
- 4) T. Sawada, H. Ninokata, et al. et al.; Validation studies of a computational model for molten material freezing, Nucl. Technol. Vol. 113, No. 2, pp.167-176, (1996).
- 5) T. Sawada, Computational modeling and verification for hexcan wall failure under simulated core disruptive accident condition, Annals of Nucl. Energy, Vol. 28, pp. 1457-1468, (2001)
- 6) G. Fieg, P. Henkel, et al.; Freezing phenomena of flowing melts in nonmelting and melting tubes, Science and technology of fast reactor safety, BNES, London, pp. 335-338, (1986).
- 7) C. R. Bell, Breeder reactor safety-Modeling the impossible," Los Alamos Science, Vol. 2, No. 2, pp. 98-11, (1981).
- 8) R. O. Gauntt and P. S. Pickard, In-pile fuel freezing and penetration experiments-the ACRR

- TRAN experiments, Science and technology of fast reactor safety, BNES, London, pp. 433-438, (1986).
- 9) R. O. Gauntt et al.; Analysis of the TRAN In-Pile fuel freezing/penetration experiments, Proc. of the int'l topical meeting on FRS, Knoxville, Tennessee, pp. 849-855, (1985).
  - 10) B.W. Spencer, R. E. Henry, et al.; "Summary and evaluation of reactor-material fuel freezing tests," Proc. of the International Meeting on Fast Reactor Safety Technol., Seattle, Washington, pp.1766-1775, (1979).
  - 11) D. A. McArthur, N. Hyden, et al.; The TRAN experiment series in the Sandia ACRR facility, Proc. of the LMFBR safety topical meeting, Lyon, France, pp. 133-141, (1982).
  - 12) T. Kamil, J. Carlsson, et al.; Comparison of sodium and lead-cooled fast reactors regarding reactor physics aspects, severe safety and economical issues, Nuclear Engineering and Design, Vol. 236, pp.1589–1598, (2006).
  - 13) M. M. Rahman, T. Hino, et al.; Experimental study on freezing behavior of molten metal on structure, Memoirs of the Faculty of Engineering, Kyushu University., Vol. 65, No. 2, pp. 85-102, (2005).
  - 14) K.H. Bang, J. M. Kim, et al.; Experimental study of molten jet break-up in water, J. Nucl. Sci. Technol., Vol. 40, No. 10, pp. 807-813, (2003).
  - 15) W. Liu, G. X. Wang and E. F. Matthys, Thermal analysis and measurements for a molten metal drop impacting on a substrate: cooling, solidification and heat transfer coefficient, International Journal of Heat and Mass Transfer, Vol. 38, No. 8, pp. 1387-1395, (1995).
  - 16) H. K. Fauske, K. Koyama, and S. Kubo, Assessment of FBR core disruptive accident (CDA): The role and Application of General Behavior Principles (GBPs), Journal of Nuclear Science and Technology, Vol. 39, No. 6, pp. 615-627, (2002).
  - 17) M. Kölling and U. Grigull, Wärme-und Stoffübertragung (Berlin), 14, P.231 (1980).
  - 18) D. Khun, M. Möschke, and H. Werle, Freezing of Aluminium oxide and Iron Flowing Upward in Circular Quartz Glass Tubes, KFK3592, Kernforschungszentrum Karlsruhe (1983).
  - 19) Y. Abe, E. Matsuo, et al.; Fragmentation behavior during molten material and coolant interactions, Nucl. Eng. and Design, Vol. 236, pp. 1668–1681, (2006).